GEOPHYSICAL RESEARCH LETTERS, VOL. 27, NO. 15, PAGES 2221-2224, AUGUST 1, 2000

Modeling of nitrogen species measured by CRISTA

M. Riese[1], V. Küll[1], X. Tie[2], G. Brasseur[3], D. Offermann[1],
G. Lehmacher[4], and A. Franzen[5]

Abstract. We present an analysis of odd nitrogen species measured by the CRISTA experiment during the Space Shuttle mission STS 66 in November 1994. Observations of several nitrogen species are compared with modeled fields obtained from three-dimensional simulations performed with a chemical transport model (CTM). A sequential trace gas assimilation system is used in order to constrain the simulations by CRISTA observations of long-lived species, and total amounts of stratospheric nitrogen (NO_y) derived from measurements of individual nitrogen components (NO_2, N_2O_5, HNO_3, and $ClONO_2$). Comparisons of measured and modeled NO_y species focus on significant diurnal variations and intense longitudinal variations observed by CRISTA.

1. Introduction

Stratospheric ozone losses primarily result from catalytic cycles involving odd nitrogen, odd chlorine, odd hydrogen, and odd bromine. Reactions involving odd nitrogen (NO_x = NO + NO_2) species are the dominant stratospheric ozone sink around ~25 km altitude [e.g. *Crutzen,* 1970]. For this reason, a detailed understanding of the partitioning of the nitrogen family is crucial for quantitative determinations of ozone destruction rates. The nitrogen partitioning can be significantly influenced by heterogeneous reactions [e.g. *Solomon et al.,* 1996]. For example, heterogeneous hydrolysis of N_2O_5 is an important sink of NO_x in the lower stratosphere [e.g. *Fahey et al.,* 1993]. The reaction also substantially alters the effect of other cycles since the ratios of odd hydrogen members (OH/HO_2) and of odd chlorine members ($ClO/ClONO_2$) are controlled by NO_x.

Analyses of the nitrogen partitioning have been performed based on aircraft and balloon observations with limited geographical coverage [e. g. *Salawitch et al.,* 1994; *Sen et al.,* 1998]. The results suggest that the partitioning of NO_y species relevant for stratospheric ozone destruction is reasonably understood, at least for conditions with high aerosol loading. Analyses of satellite data provide global coverage and reveal a gradual increase of the NO_y/NO_x ratio in the post-Pinatubo stratosphere, consistent with model predictions [e. g. *Morris et al.,* 1997; *Danilin et al.,* 1999]. However, to date the nitrogen partitioning obtained from satellite observations has only be investigated in terms of zonally averaged values or single profile data based on box models or two-dimensional models.

This paper presents three-dimensional simulations of nitrogen species obtained from the first flight of the Cryogenic Infrared Spectrometers and Telescopes for the Atmosphere (CRISTA) experiment in early November, 1994. A sequential trace gas assimilation technique is used to constrain simulations of individual nitrogen species by measured distributions of long-lived species and by total amounts of stratospheric nitrogen (NO_y) derived from CRISTA observations of individual nitrogen compounds. The observations are assimilated into a three-dimensional chemical transport model (CTM), which combines the chemistry and the transport codes of the NCAR ROSE model [e. g. *Rose and Brasseur,* 1989] with analyzed wind and temperature fields provided by the U. K. Meteorological Office (UKMO) [*Swinbank and O'Neill,* 1994]. Through this approach, the simulations account for the dynamical conditions prevalent during the observation period of CRISTA.

2. Observations

The CRISTA instrument uses the limb-scanning technique to measure global distributions of thermal emissions of selected trace gases. For high horizontal resolution three telescopes are used that sense the atmosphere simultaneously. The vertical resolution of the measurements is about 2.5 km. The measurement technique allows observations during both daytime and nighttime.

The first flight of the instrument was performed during the Space Shuttle mission STS 66 in November, 1994 [*Offermann et al.,* 1999; *Riese et al.,* 1999a]. The instrument was operated for eight days (November 4-12, 1994) and provided atmospheric distributions of numerous trace gases with unprecedented horizontal resolution for a limb-scanning instrument (typically 6° in longitude and 3° in latitude). Previous stratospheric studies based on CRISTA observations have used measured values of O_3, CH_4, N_2O, CFC-11, HNO_3, and $ClONO_2$. The present analysis includes, in addition, observations of NO_2 and N_2O_5.

For analyses of chemically active species it is especially important to consider the local solar time (LST) distribution of the observations. Figure 1 shows solar local times for the center

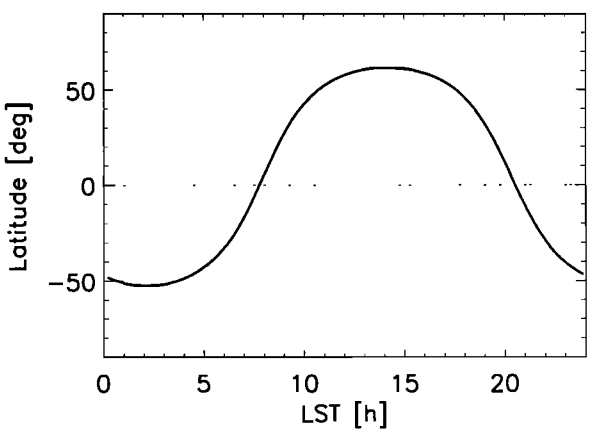

Figure 1. Local solar time (LST) distribution of the center telescope at points around an orbit for November 9, 1994.

[1]Physics Department, University of Wuppertal, Wuppertal, Germany
[2]National Center for Atmospheric Research, Boulder, Colorado
[3]Deutsches Klimarechenzentrum, Hamburg, Germany
[4]Now at Western Kentucky University, Bowling Green, Kentucky
[5]Now at Bull GmbH, Langen, Germany

Copyright 2000 by the American Geophysical Union.

Paper number 1999GL011136.
0094-8276/00/1999GL011136$05.00

telescope at points around an orbit for Nov. 9, 1994 (day 313). Measurements at the ascending portion (upleg) were made mainly during daytime, while measurements at the descending portion (downleg) were made mainly during nighttime. At each latitudinal circle, observations of each telescope were obtained at two different local solar times (LST) with a maximum local time difference of 12 hours at the equator. However, observations in the latitudinal region of the northern and southern turning points of the orbital track provide information over a relatively large portion of the diurnal cycle. In addition, the LST shifts by –22 minutes per day at a given latitude and the LST sampling of the three telescopes is somewhat different.

The sequential trace gas assimilation system uses a horizontal resolution of 2.5° in latitude and 5.6° in longitude, and a vertical resolution of about 2.7 km. Due to the high spatial resolution of CRISTA, trace gas concentrations are frequently updated at all model grid points inside the atmospheric region sampled by the instrument. Details of the assimilation of long-lived species are given by *Riese et al.*, 1999b. The next section describes an extension of the trace gas assimilation technique to chemical families (NO_y, Cl_x, O_x), which is used in order to constrain simulations of chemically active species such as N_2O_5 and NO_2.

3. Sequential data assimilation

The assimilation is based on the "observed" densities of families, which are estimated from measurements of individual components. The reactive nitrogen reservoir (NO_y) is estimated, for example, from the observed nitrogen components (NO_y^i) and the relative contribution of each component to total NO_y as predicted by the model (hereafter α_i). The model predictions of the nitrogen partitioning are evaluated at the locations (altitude z, longitude λ, latitude ϕ) and the local solar times (LST) of the observations. An estimate of the "observed" NO_y amount (NO_y^i/α_i) is performed for each measured nitrogen component NO_y^i. The best estimate of the "observed" NO_y value is obtained by weighting the different estimates inversely with their errors σ^2. Finally, best estimate for NO_y is inserted into the model by the sequential assimilation procedure.

Since the observed NO_y members (NO_2, HNO_3, N_2O_5, and $ClONO_2$) are not directly inserted into the model, their values will only be in good agreement with corresponding model results, if the partitioning ratios predicted by the model are in good agreement with the partitioning ratios measured by CRISTA.

The model predictions of the nitrogen partitioning are basically a function of the atmospheric aerosol loading and kinetic parameters of key gas-phase reactions (e. g. R_1: $NO_2 + OH + M \rightarrow HNO_3$; R_2: $OH + HNO_3 \rightarrow NO_3 + H_2O$). As discussed by *Osterman et al.*, [1999], gas-phase kinetic parameters of *DeMore et al.*, [1994] result in better agreement between modeled and observed nitrogen species than kinetic parameters provided by *DeMore et al.*, [1997], mainly due to a slower rate of reaction R_1. Recent studies [e.g. *Gao et al.*, 1999] demonstrate that best agreement is achieved when using newly measured rate constants [*Brown et al.*, 1999a,b] for reactions R_1 and R_2.

To test the sensitivity of the modeled nitrogen species to the aerosol loading and to the values of the kinetic parameters, four test cases have been defined: Case A_1 is based on the newly measured rate constants and on aerosol surface densities obtained from SAGE II observations during October, 1994; for case A_2 heterogeneous reactions are neglected; case B_1 uses the newly measured rate constants and aerosol loading measured by HALOE; case B_2 is based on HALOE aerosol and kinetic parameters of the JPL-94 compilation.

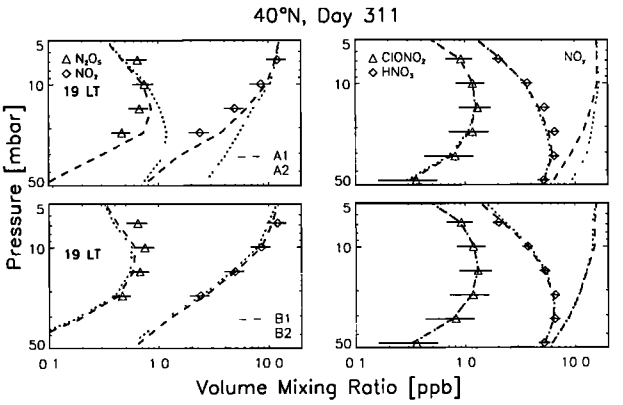

Figure 2. Comparison of measured (symbols) and simulated zonal mean profiles (30°N to 50°N) of nitrogen components for early nighttime conditions (19 LT). The left panel shows results for N_2O_5 and NO_2, while the right panel shows $ClONO_2$, HNO_3, and NO_y values. For details concerning the model cases A_1, A_2, B_1, and B_2 see text.

Comparisons of measured (symbols) and modeled (lines) mixing ratio profiles of four nitrogen components are presented in Figure 2. Midlatitude (30°N to 50°N) zonal averages calculated from individual profile measurements and corresponding forecasts of the constrained model are shown for early nighttime conditions (19 LST). The upper panel of Figure 2 demonstrates the importance of heterogeneous reactions on sulfate aerosols at altitudes below 10 mbar (30 km). The neglect of heterogeneous reactions in case A_2 results in a considerable overestimate of the amount of N_2O_5 and NO_2. More realistic results are obtained in cases A_1 and B_1. Compared to the large influence of the aerosol loading assumed for the simulations, the sensitivity of N_2O_5 and NO_2 to assumptions made for the gas-phase rate constants (case B_2) is rather small. In the next section some results of case B_1 are discussed in terms of significant diurnal variations and large horizontal variations.

4. Results and Discussion

The local solar time (LST) distribution shown in Figure 1 indicates that most information about diurnal variations of chemically active species is contained in observations performed in the latitudinal region of the northern and southern turning points of the orbital tracks. Figure 3a shows CRISTA values of NO_2 at 3.16 mbar measured during Nov. 7 (day 311) in the latitudinal band from 50°N to 60°N (red points). Note that observations of other nitrogen species are not available at this altitude level. The LST coverage of the combined measurements includes the day to night transition (terminator), where steep gradients in the diurnal variation of NO_2 occur. The large scatter of the observations is mainly due to latitudinal gradients and intense zonal variations caused by dynamical processes. The CRISTA observations were performed during a dynamically disturbed period characterized by large wave activity and exchange of tropical and extratropical air in form of planetary-scale tongues (see e. g. Plates 6 and 7 of Riese et al., 1999b). Figure 3a also shows observed values averaged over the time step of the model (black symbols). The observations are compared to a zonally averaged diurnal cycle obtained from the model (red line). The night/day ratio is of the order of 3-4 for

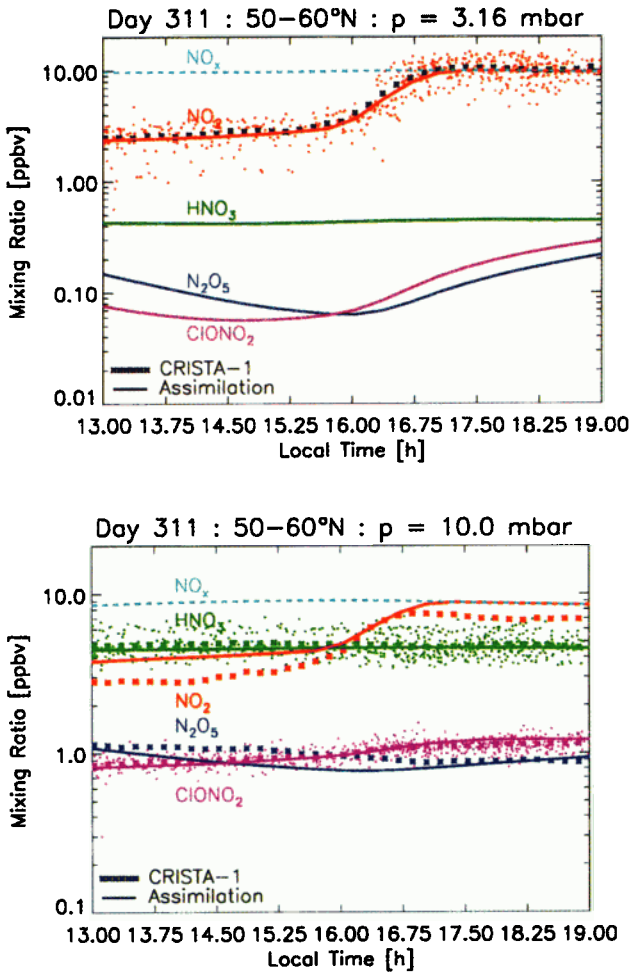

Figure 3. **(a)** Comparison of measured and modeled diurnal variations of nitrogen species at 3.16 mbar (50°N to 60°N). Single observations of NO_2 are given by red points. Mean observed NO_2 values are also shown (black symbols). Corresponding zonally averaged model results are given by colored lines (red: NO_2, green: HNO_3, blue: N_2O_5, violet: $ClONO_2$). For more details see text. **(b)** Same as Figure 3a but for the 10 mbar level. Single observations are shown for HNO_3 (green points) and $ClONO_2$ (violet points). Mean observed values are shown for all species (colored symbols).

both model results and observations. Simulated values of unmeasured species such as NO_x (NO_2 + NO), HNO_3, $ClONO_2$, and N_2O_5 are also shown in Figure 3a. Figure 3b presents the same comparison but for the 10 mbar level, where CRISTA observations of NO_2, HNO_3, N_2O_5, and $ClONO_2$ are available. Shown are averaged values for all species (colored symbols) as well as single observations of HNO_3 (green points) and $ClONO_2$ (violet points). At this pressure level, the night/day ratio is larger in the observation than in the model.

Comparisons of horizontal distributions of measured and modeled NO_y species are presented in Figure 4 for Nov. 6 (day 310) at 22.5 mbar. The left panel shows the observation, while the right panel shows the model forecast at the instrument sampling grid, i. e. at the locations and times of the observations. The HNO_3 distributions (upper panel) contain all measurement points of Nov. 6 (upleg and downleg), since no major diurnal variations are present at this altitude level. $ClONO_2$ observations on the upleg were separated from observations on the downleg (2nd and 3rd panel). For N_2O_5 (lowest panel), only measurements on the downleg are given. The model well reproduces the shape of the polar vortex in the HNO_3 distribution. In the northern hemisphere two pronounced planetary-scale tongues can be seen in both observations and model results. Another weaker tongue of tropical air extends across the South American continent into the Indian Ocean. The overall agreement of the observed and the modeled structures is remarkable. The most notable difference is the overestimation of HNO_3 by the model in the tropics. The observed $ClONO_2$ distributions exhibit important diurnal variations, which are well reproduced by the model. The model also reproduces significant horizontal structures at middle latitudes, which resemble the structures observed in HNO_3. For N_2O_5, the overall agreement is considerably worse. In particular, the model overestimates the amount of N_2O_5 at high latitudes, probably due to an underestimate of the aerosol loading. This

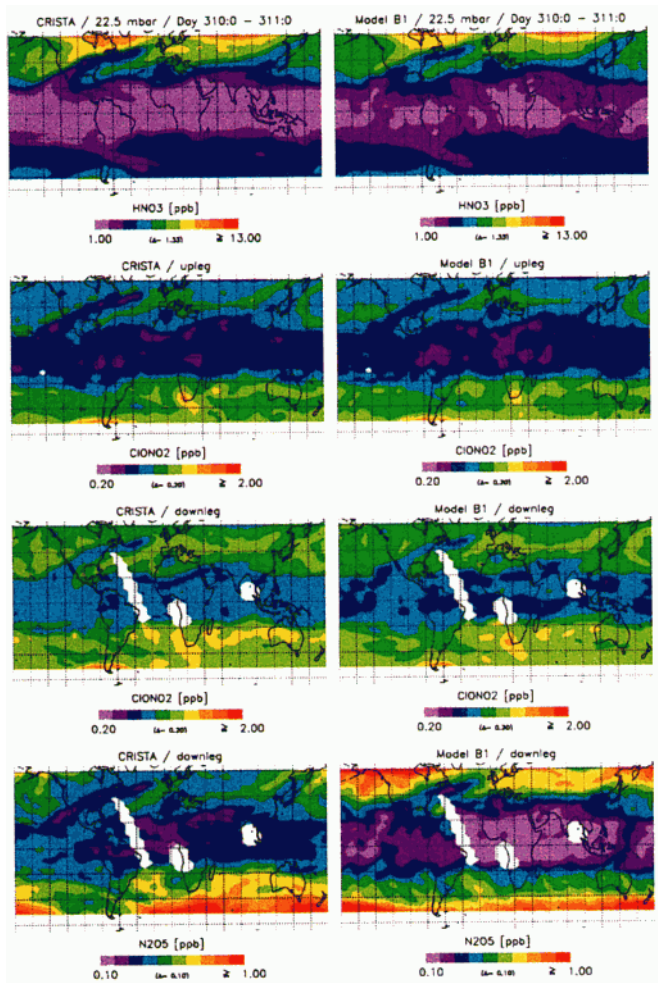

Figure 4. Comparison of measured and modeled nitrogen species for Nov. 6, 1994, at 22.5 mbar. Shown are distributions of HNO_3, $ClONO_2$ (upleg), $ClONO_2$ (downleg), and N_2O_5 (downleg). The distributions were obtained by interpolating the trace gas values onto a regular grid with 64 x 72 grid points (longitude x latitude). The interpolation has been performed by applying a two-dimensional weighting function, which resembles a triangle function with a half width of 8° in longitude and 4° in latitude. Blank areas indicate grid points where no measured data are available inside the nonzero region of the weighting function. For more details see text.

discrepancy becomes even larger when aerosol surface densities provided by SAGE II (case A_1) are used.

In general, good correspondence between measured and observed structures is found. Sequential assimilation of chemical families appears to be an attractive method to analyze satellite observations of short-lived species, especially to check on our understanding of photochemical processes involving individual family members.

Acknowledgments. We wish to thank L. L. Gordley and T. B. Marshall of Gordley Associated Software for supporting the CRISTA trace gas retrieval. We also thank the SAGE II and HALOE teams for providing aerosol surface densities via world wide web. The CRISTA project was supported by grant 50 OE 8501 of Deutsche Agentur für Weltraumangelegenheiten (DARA), Bonn, Germany. The work of X. Tie is supported by the DOE Atmospheric Chemistry Program under contract DE-AI05-94ER619577. The National Center for Atmospheric Research is sponsored by the National Science Foundation.

References

Brown, S. S., R. K. Talukdar, and A. R. Ravishankara, Rate constants for the reactions $OH+NO_2+M \rightarrow HNO_3+M$ under atmospheric conditions, *Chem. Phys. Lett., 299,* 277-284, 1999a.

Brown, S. S., R. K. Talukdar, and A. R. Ravishankara, Reconsideration of the rate constant for the reaction of hydroxyl radicals with nitric acid, *J. Phys. Chem., 103,* 3031-3037, 1999b.

Crutzen, P. J., The influence of nitrogen oxides on the atmospheric ozone content, *J. R. Meteorol. Soc., 96,* 320-325, 1970.

Danilin, M. Y. et al., Nitrogen species in the post-Pinatubo stratosphere: Model analysis utilizing UARS measurements, *J. Geophys. Res.,* 104, 8247-8262, 1999.

DeMore, W. B. et al., Chemical kinetics and photochemical data for use in stratospheric modeling, *JPL Pub. 94-26,* 1994.

Be More, W. B. et al., Chemical kinetics and photochemical data for use in stratospheric modeling, *JPL Publ. 97-4,* 1997.

Fahey, D. W., et al, In situ measurements constraining the role of sulfate aerosols in mid-latitude ozone depletion, *Nature, 363,* 509-514, 1993.

Gao, R. S., et al., A comparison of observations and model simulations of NO_x/NO_y in the lower stratosphere, *Geophys. Res. Lett., 26,* 1153-1156, 1999.

Morris, G. A., D. B. Considine, A. E. Dessler, S. R. Kawa, J. Kumer, J. Mergenthaler, A. Roche, and J. M. Russell III, Nitrogen partitioning in the middle stratosphere as observed by the Upper Atmosphere Research Satellite, J. Geophys. Res., 102, 8955-8965, 1997.

Offermann, D., K. U. Grossmann, P. Barthol, P.Knieling, M. Riese, and R. Trant, Cryogenic Infrared Spectrometers and Telescopes for the Atmosphere (CRISTA) experiment and middle atmosphere variability, *J. Geophys. Res., 104,* 16,311-16,325, 1999.

Osterman, G. B., B. Sen, G. C. Toon, R. J. Salawitch, J. J. Margitan, J.-F. Blavier, D. W. Fahey, and R. S. Gao, Partitioning of NO_y species in the summer Arctic stratosphere, *Geophys. Res. Lett., 26,* 1157-1160, 1999.

Riese M., R. Spang, P. Preusse, M. Ern, M. Jarisch, D. Offermann, and K. U. Grossmann, Cryogenic Infrared Spectrometers and Telescopes for the Atmosphere (CRISTA) data processing and atmospheric temperature and trace gas retrieval, *J. Geophys. Res., 104,* 16,349-16367, 1999a.

Riese M., X. Tie, G. Brasseur, and D. Offermann, Three-dimensional simulations of stratospheric trace gas distributions measured by CRISTA, *J. Geophys. Res., 104,* 16,419-16,435, 1999b.

Rose, K. and G. Brasseur, A three-dimensional model of chemically active trace species in the middle atmosphere during disturbed winter conditions, *J. Geophys. Res., 96,* 16,387-16,403, 1989.

Salawitch, R. J., et al., The distribution of hydrogen, nitrogen, and chlorine radicals in the lower stratosphere: Implications for changes on O_3 due to emissions of NO_y from supersonic aircraft, *Geophys. Res. Lett., 21,* 2547-2550, 1994.

Sen, B., G. C. Toon, G. B. Osterman, J.-F. Blavier, J. J. Margitan, R. J. Salawitch, and G. K. Yue, Measurements of nitrogen in the startosphere, *J. Geophys. Res., 103,* 3571-3585, 1998.

Solomon, S., R. W. Portmann, R. R. Garcia, L. W. Thomason, and M. P. McCormick, The role of aerosol variations in antropogenic ozone depletion at northern midlatitudes, *J. Geophys. Res., 101,* 6713-6727, 1996.

Swinbank, R. and A. O'Neill, A stratosphere-troposphere data assimilation system, *Mon. Weather Rev., 82,* 686-702, 1994.

M. Riese, V. Küll, and D. Offermann, University of Wuppertal, Gauss-Str.20, 42097 Wuppertal, Germany
(e-mail: riese@wpos2.physik.uni-wuppertal.de)

X. Tie, National Center for Atmospheric Research, Boulder, Colorado (e-mail: xxtie@acd.ucar.edu)

G. Brasseur, Deutsches Klimarechenzentrum, Hamburg, Germany (e-mail: brasseur@dkrz.de)

G. Lehmacher, Western Kentucky University, Bowling Green, Kentucky (e-mail: Gerald.Lehmacher@wku.edu)

A. Franzen, Bull GmbH, Langen, Germany
(e-mail: a.franzen@bull.de)

(Received October 1, 1999; revised March 22, 2000;
accepted May 22, 2000.)